Petroleum Science 21 (2024) 1211–1220

Contents lists available at ScienceDirect

Petroleum Science

journal homepage: www.keaipublishing.com/en/journals/petroleum-science

Original Paper

Evaluation of the injection and plugging ability of a novel epoxy resin in cement cracks

Guang-Yao Leng [a], Wei Yan [a, *], Hai-Mu Ye [a], Er-Dong Yao [a], Ji-Bin Duan [b], Zheng-Xian Xu [a], Ke-Pei Li [a], Jing-Ru Zhang [a], Zhong Li [a, c]

[a] State Key Laboratory of Petroleum Resource & Prospecting, China University of Petroleum (Beijing), Beijing, 102249, China
[b] CNPC Liaohe Oilfield Gas Storage Co. LTD, Panjin, 124000, Liaoning, China
[c] CNOOC Research Institute Co., Ltd., Beijing, 100028, China

ARTICLE INFO

Article history:
Received 31 March 2023
Received in revised form
18 October 2023
Accepted 18 October 2023
Available online 19 October 2023

Edited by Jia-Jia Fei

Keywords:
Sustained casing pressure
Epoxy resin sealant
Curing agent
Viscosity reducer
Mechanical properties
Crack sealing

ABSTRACT

Sustained casing pressure (SCP) is a crucial issue in the oil and gas production lifecycle. Epoxy resins, exhibiting exceptional compressive strength, ductility, and shear bonding strength, have the potential to form reliable barriers. The injectivity and sealing capacity of the epoxy resin is crucial parameters for the success of shallow remediation operations. This study aimed to develop and assess a novel solid-free resin sealant as an alternative to Portland cement for mitigating fluid leakage. The investigation evaluated the viscosity, compressive strength, and brittleness index of the epoxy resin sealant, as well as its tangential and normal shear strengths in conjunction with casing steel. The flow characteristics and sealing abilities of conventional cement and epoxy resin were comparatively analyzed in cracks. The results showed that the application of a viscosity reducer facilitated control over the curing time of the epoxy resin, ranging from 1.5 to 6 h, and reduced the initial viscosity from 865.53 to 118.71 mPa•s. The mechanical properties of the epoxy resin initially increased with a rise in curing agent content before experiencing a minor decrease. The epoxy resin containing 30% curing agent exhibited optimal mechanical properties. After a 14-day curing period, the epoxy resin's compressive strength reached 81.37 MPa, 2.12 times higher than that of cement, whereas the elastic modulus of cement was 2.99 times greater than that of the epoxy resin. The brittleness index of epoxy resin is only 3.42, demonstrating high flexibility and toughness. The tangential and normal shear strengths of the epoxy resin exceeded those of cement by 3.17 and 2.82 times, respectively. In a 0.5 mm-wide crack, the injection pressure of the epoxy resin remained below 0.075 MPa, indicating superior injection and flow capabilities. Conversely, the injection pressure of cement surged dramatically to 2.61 MPa within 5 min. The breakthrough pressure of 0.5 PV epoxy resin reached 7.53 MPa, decreasing the crack's permeability to 0.02 D, a mere 9.49% of the permeability observed following cement plugging. Upon sealing a 2 mm-wide crack using epoxy resin, the maximum breakthrough pressure attained 5.47 MPa, 3.48 times of cement. These results suggest that epoxy resin sealant can be employed safely and effectively to seal cracks in the cement.

1. Introduction

The integrity of cement sheath sealing is crucial to the safe operation of wellbores (Du et al., 2020; Guo et al., 2020a; Li et al., 2022). The cement sheath, as a barrier between the casing and the formation, must effectively prevent fluid migration along the annular space (Alkhamis and Imqam, 2018). However, cement is susceptible to brittle failure due to pressure and temperature fluctuations, as well as mechanical and chemical corrosion, resulting in microcracks or cracks. These defects may cause a reduction or failure of the cement sheath integrity, resulting in sustained casing pressure (SCP) in the wellbore's annular space (Ahdaya and Imqam, 2019). SCP is regarded as a significant challenge in global oil and gas well integrity management (Gu et al., 2022; Skadsem, 2022a, b; Zhu et al., 2012). According to a 2003 report by the US Bureau of Land Management, SCP has affected over

* Corresponding author.
E-mail address: yanwei@cup.edu.cn (W. Yan).

https://doi.org/10.1016/j.petsci.2023.10.014

8000 oil and gas wells in the Gulf of Mexico region (Rusch, 2004).

Squeeze cementing is a prevalent remedial technique in shallow remediation operations (Jelena et al., 2016; Manceau et al., 2014), involving the injection of cement into cement cracks or poorly bonded areas to obstruct fluid migration pathways. This method presents some limitations, including void size, particle fluid seepage, and migration pathway obstruction (Jones et al., 2014). Multiple squeezes or different squeeze techniques, such as hesitation squeezing, may be required to address these issues (Alkhamis and Imqam, 2021; Sanabria et al., 2016). In addition, there are some obstacles during the cementing process, including low injection capacity, high injection pressure, and internal microcracks in the primary cement (Ali et al., 2022).

Sealant injection in the annulus is a prevalent technique for shallow remediation in SCP repair, aiming to improve annular zonal isolation. The injectivity and sealing capability of the sealant are vital success factors for this operation (Elyas et al., 2018). The sealant must be able to migrate over great distances in microcracks or leak channels and withstand formation or wellbore gas pressure. Sealants such as microfine cement, ultrafine cement, polymer gels, and polymer resins are currently the subject of extensive research and application. Even though various sealants have had some success in practical applications, they also exhibit some limitations. Fine and ultrafine cement, for instance, struggle to penetrate pores narrower than 300 μm and are susceptible to contamination (Dahlem et al., 2017; Wasnik and Mete, 2005). In addition, casing perforation is frequently required for this operation. Polymer gels are liquid-to-semisolid transforming mixtures of polymers and crosslinking agents with the ability to penetrate small voids; however, their mechanical strength and bonding performance are significantly limited (Abdulfarraj and Imqam, 2020).

Epoxy resin is a thermosetting polymer with exceptional adhesion and strength, comprising base epoxy resin and a curing agent (Fan et al., 2022). It is characterized as a "free-flowing polymer solution that can be irreversibly cured into a hard solid" (Marfo et al., 2015). Epoxy resin solution exhibits variable rheological behavior and lacks solid phases, resulting in outstanding flowability. It can infiltrate small cracks and exhibit effective performance in crack repair (Alsaihati et al., 2017; Todd et al., 2018). Compared to cement, cured epoxy resin possesses a lower elastic modulus, greater compressive strength, and superior bonding performance (Al-Yami et al., 2019; Huseien et al., 2021). Guo et al. (2020b) observed that the polymer film produced by epoxy resin can enhance the microstructure of OPC mortar. Ren et al. found that TiO_2/epoxy resin composites can enhance the mechanical properties such as compressive and flexural strength of AASF paste, and proposed strengthening mechanisms including the epoxy resin bridging effect and pore-filling effect (Guo et al., 2021a, b; Ren et al., 2020). Song reported that the elastic modulus of cement-based composites containing 30% resin decreased by 63.2% after 28 days of curing (Song et al., 2022). Schütz et al. (2019) studied the CO_2 chemical resistance of class G cement modified with 1% and 2.5% epoxy resin. Albertus discovered that the optimal concentration of resin added to class G cement slurry is 7.5%, resulting in a 52% increase in compressive strength (Retnanto et al., 2023). Existing studies have primarily focused on epoxy resin-cementitious composite materials, leaving limited research on the injection capacity and sealing efficiency of epoxy resin through poorly bonded interfaces or cracks. Additionally, the viscosity, curing time, and plugging capability of epoxy resin are closely related to the concentrations of curing agent and viscosity reducer used.

To achieve optimal performance, the design and preparation of epoxy resin sealants must consider the impact of the aforementioned parameters on plugging efficiency and injection capacity. In the present study, a flexible epoxy resin sealant capable of curing at low temperatures was synthesized in the laboratory. The epoxy resin and conventional cement sealants were comparatively assessed based on compressive strength, tangential shear strength, normal shear strength, and brittleness index. Additionally, the injection capacity and plugging efficiency of the sealant in cracks were evaluated, offering technical support for shallow SCP remediation.

2. Experimental description

2.1. Materials

Oilwell cement (class G Portland cement) was procured from the Jiahua Special Cement Co. Ltd., Leshan, China. Epoxy resin E51 (epoxy value 0.48–0.54 eq/100 g, viscosity roughly 12000 mPa·s at 25 °C) was obtained from Xingchen Synthetic Materials Co. Ltd., Nantong, China. Polyetheramine D230 (total amine value 0.2 meq/g, viscosity 9.5 mPa·s at 25 °C) was produced by Shengxu Energy Co. Ltd., Shandong, China. Phenalkamine NX-2003 (amine value 330–375 mg KOH/g, viscosity 500–1300 mPa·s at 25 °C) was obtained by Cardolite Chemicals (Zhuhai) Co. Ltd., Guangdong, China. Butyl glycidyl ether BGE (epoxy value$\geq$0.5 eq/100g, viscosity$\leq$2 mPa s at 25 °C) was produced by Sinopharm Chemical Reagent Co. Ltd., Shanghai, China.

2.2. Sealant preparation

This study involved the preparation of two sealants, including conventional cement and epoxy resin systems. By American Petroleum Institute (API) specification 10A (Schütz et al., 2018), the cement slurry (S-0) was prepared with a constant water-to-cement ratio of 0.44, and the curing age ranged between 3 and 14 days.

To determine the impact of the curing agent and viscosity reducer BGE content on the epoxy resin system's performance, three mass ratios of epoxy resin to curing agent were established: 100:20 (S-1), 100:30 (S-2), and 100:40 (S-3). The curing agent comprises D230 and NX2003 in a 3: 1 mass ratio. The proportion of viscosity reducer relative to the total quantity of epoxy resin and curing agent ranges from 0% to 15%. E-51 is a bifunctional epoxy resin known for its excellent mechanical and thermal properties. A 100 mL beaker was placed on an analytical balance. A predetermined amount of epoxy resin was transferred to the beaker using a disposable transfer pipette, followed by uniform stirring. Another disposable transfer pipette was used to introduce the viscosity reducer into the beaker and stirred until fully mixed. The curing agent was added and stirred at a low shear rate until a homogeneous mixture was achieved, which was then transferred to a sample container. The mixture was immediately cured in a 30 °C water bath, resulting in the formation of a bisphenol A-type epoxy resin.

2.3. Viscosity test

When the consistency of epoxy resin reaches 100 Bc, unlike cement materials, its fluidity is still greater than 20 cm (Cao et al., 2022). Epoxy resin liquid exhibits favorable flow properties. The viscosity of the epoxy resin was measured in this study using a Brookfield DV–II viscometer (Brookfield, United States). Given the temperature sensitivity of epoxy resin viscosity, a water bath circulation system was employed to maintain a consistent temperature during measurements. Following a 30-min instrument stabilization period, data collection commenced by the GB/T 7193–2008 standard. Appropriate rotor types were selected based on actual viscosity values, ensuring readings fell within 20% and 90% of the full scale. Each data point represents the average of three

measurements. The experimental setup evaluated the impact of the viscosity reducer on the epoxy resin sealant's viscosity, using a resin-to-curing agent mass ratio of 100:30.

2.4. Mechanical properties test

2.4.1. Compressive strength

The compressive strength of epoxy resin and cement sealants is a critical parameter for evaluating their capacity to withstand demanding downhole environments. The elastic modulus, defined as the stress-to-strain ratio, is a material property that characterizes a material's resistance to deformation. In compliance with GB/T 50266−2013, the compressive strength and elastic modulus of the cured sealant were determined by coring and grinding samples into cylinders with a diameter of 25 mm and a length of 50 mm. High-precision displacement sensors were fitted in both axial and radial directions of the sealant samples. A TAW1000 pressure experimental servo system was utilized to measure the strain of the sealant under uniaxial stress loading. Fig. 1 displays the tested cement and epoxy resin samples. The sealant samples were subjected to failure under a constant loading rate of 2 kN/min, and the outcomes of the uniaxial stress-strain tests were acquired. The sealant's elastic modulus was calculated employing the two-point method. Each experimental group comprised three replicate samples. The brittleness index of the sample was obtained by testing the flexural strength of the sample.

2.4.2. Tangential shear strength and normal shear strength

The tangential shear strength, which signifies the bond strength in the tangential direction at the casing-cement interface, is crucial for preventing such relative motion. Similarly, the normal shear strength, which evaluates the bond strength in the perpendicular direction at the interface, is essential for averting adhesive failure. To maintain the integrity of the interfacial bond, both the tangential and normal shear strengths must satisfy the designated criteria.

Fig. 2 illustrates the experimental setup and methodology employed to assess the tangential and normal shear strengths of conventional cement and epoxy resin sealant at the casing-cement interface. Within the apparatus, the cement and epoxy resin sealant was cured and subsequently compressed utilizing three solid cylinders. For the determination of tangential shear strength, the maximum failure load was documented.

Similar to the maximum failure load, the normal shear strength was measured by applying force to three rectangular metal plates. Each sealant sample was evaluated three times, and the average value was calculated. The two shear strengths were determined using the following formula :

$$\tau = \frac{P}{A} \tag{1}$$

where τ is tangential shear strength and normal shear strength (MPa), P is the failure load (N), and A is the area of the interface area (m^2) between the cement or epoxy resin and solid cylinder or rectangular metal plate.

2.5. Injectivity and plugging tests

Before SCP remediation, sealant injectivity testing is essential to determine critical parameters and limitations. This experiment's research methodology is based on the conventional core flooding scheme. A high-precision metering pump, three intermediate containers, a core holder, two pressure sensors, and a confining pressure pump are utilized in this experiment (as shown in Fig. 3). The cement core size used was 7 cm long and 2.5 cm in diameter. The cement core is split in half, with two stainless steel gaskets of equal thickness placed in the middle. The sample is then positioned within the core holder. After connecting the experimental flow, water is injected into the cement core cracks until the first drop of water exits the outlet end. The crack pore volume (PV) was determined by subtracting the internal volume of the displacement pipeline from the saturated water volume. The initial permeability of a crack can be determined by recording the pressure during water injection. Next, epoxy resin and cement sealant are separately injected into the crack at volumes equal to 0.2 and 0.5 times the crack's pore volume, respectively. After three days of curing, water is injected into the cement core. The maximum injection pressure was defined as the breakthrough pressure and water injection was continued until the pressure stabilized. The stable pressure is used to calculate the permeability. The experiment temperature is 30 °C, and the rate of water injection is 0.3 mL/min. To ensure precise measurement and stable sealant migration, the sealant injection rate is reduced to 0.1 mL/min. The impact of cement crack size on the injectivity and plugging capability of the sealing material is assessed using two different thicknesses of steel plates (0.5 and 2 mm). During all experiments, pressure data is recorded by sensors.

3. Results and discussion

3.1. Epoxy resin viscosity

To guarantee construction safety, the sealant must possess adequate liquid seepage time for pumping and positioning in the designated location during cement sheath repairs. Fig. 4 illustrates the impact of the viscosity reducer on epoxy viscosity. As the

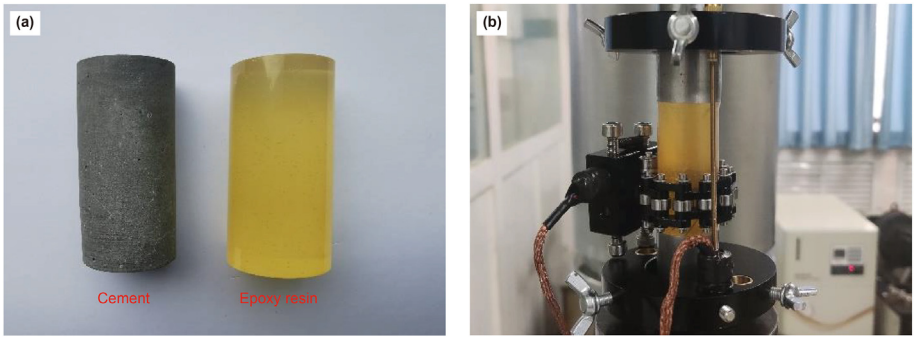

Fig. 1. Compressive strength test equipment. (**a**) Epoxy resin and cement sample. (**b**) The sample is under compressive load.

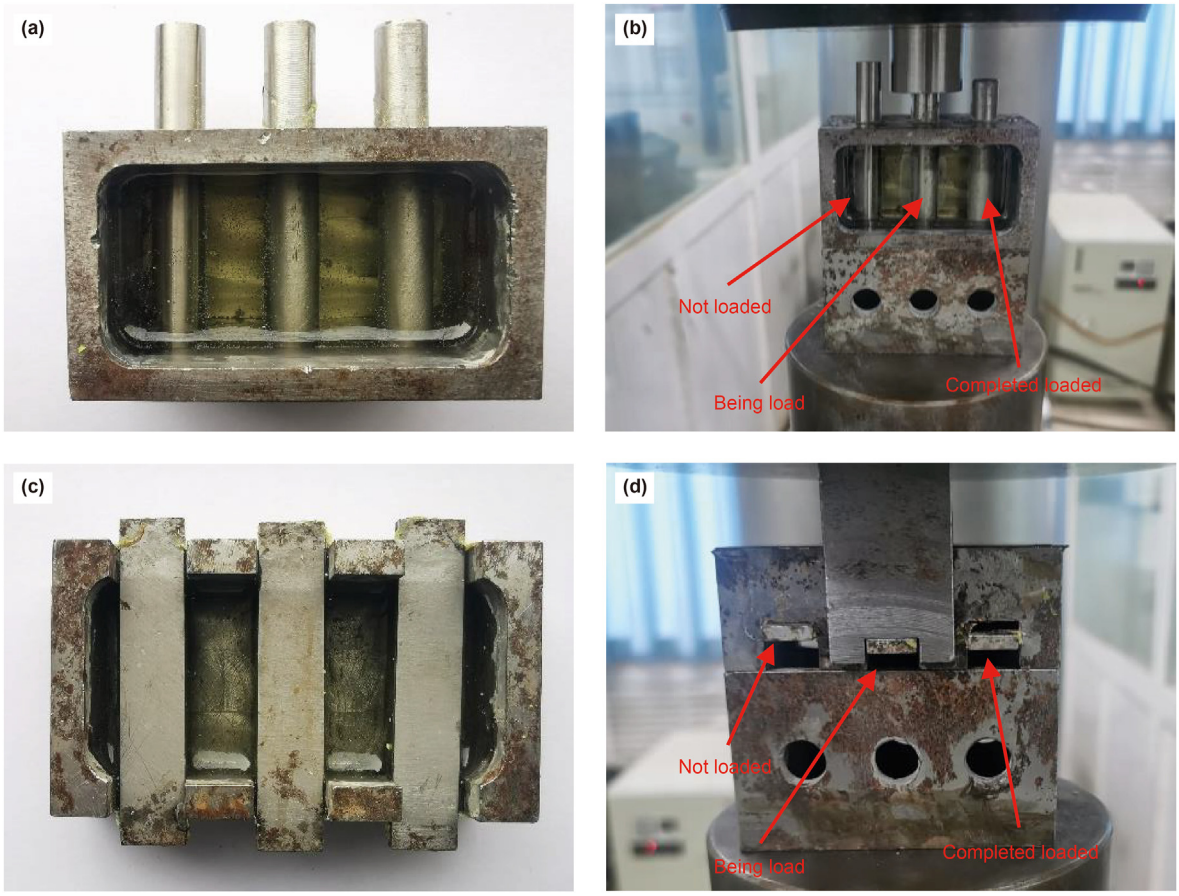

Fig. 2. The self-made equipment for the shear strength test. (**a**) Cured cement sample with three solid cylinders. (**b**) The sample was loaded to test tangential shear strength. (**c**) Cured cement sample with three rectangular metal plates. (**d**) The sample was loaded to test normal shear strength.

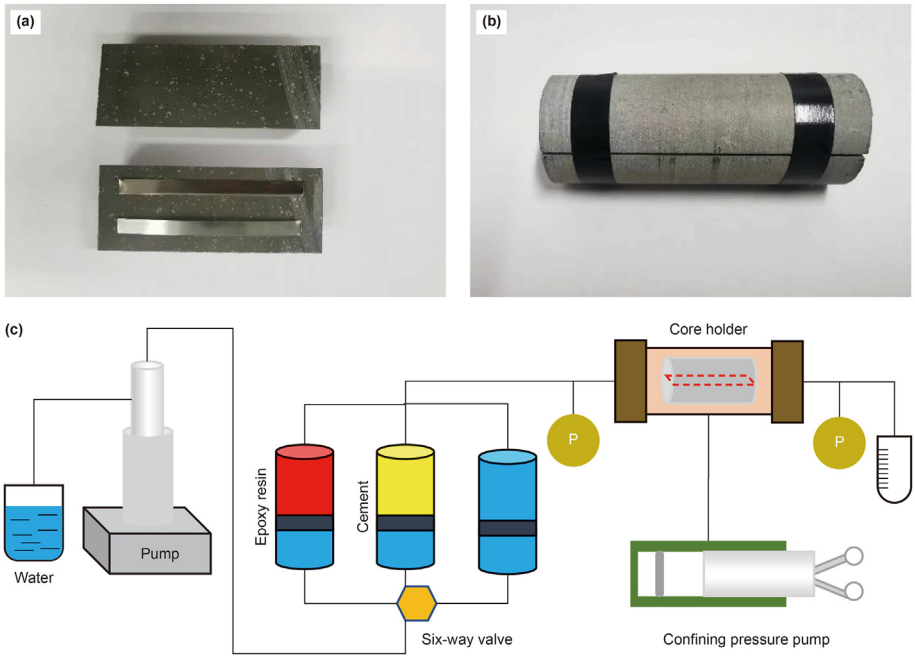

Fig. 3. Injectivity and plugging ability tests for cement and epoxy resin sealants. (**a**) Two halves of cement core with steel plates. (**b**) Cement core with simulated crack. (**c**) Experimental flow diagram.

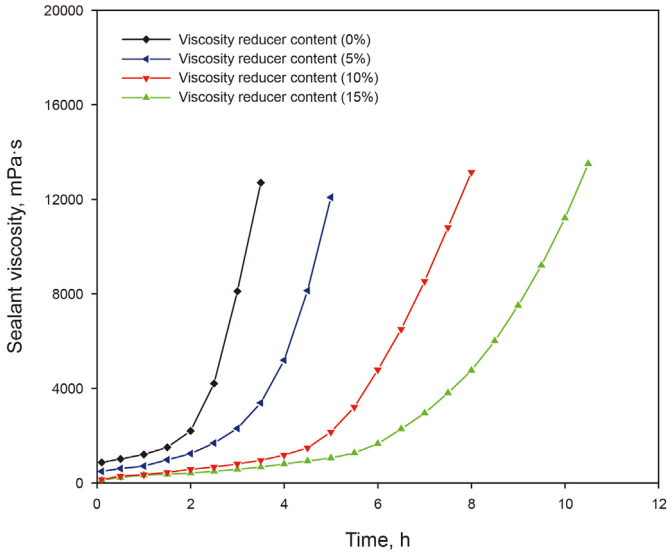

Fig. 4. Effect of viscosity reducer on the viscosity of the epoxy resin.

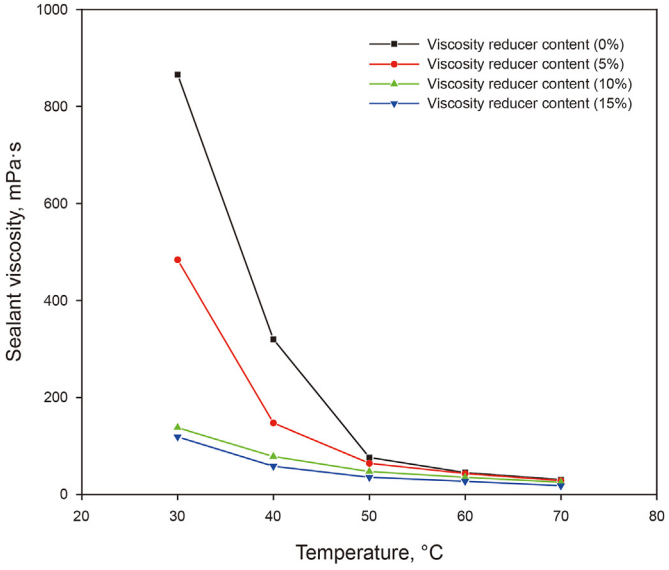

Fig. 5. Effect of temperature on the viscosity of the epoxy resin.

viscosity reducer content increases, the epoxy resin sealant's viscosity decreases. Preliminary tests indicate that the sealant's viscosity measures 865.53 mPa·s with 0% viscosity reducer and 483.72 mPa·s with 5%. The quantity of viscosity reducer is the primary determinant of the sealant's viscosity. Nevertheless, when the viscosity reducer increases from 10% to 15%, the viscosity declines from 137.52 to 118.71 mPa·s, exhibiting a diminished effect. The four curves exhibit inflection points in viscosity, showing a gradual increase before the inflection point and a steep rise thereafter, indicating an enhanced sealant-curing reaction. The curing time lengthens with increasing viscosity reducer content. As the viscosity reducer content escalates from 0% to 15%, the curing time extends from 1.5 to 6 h. The addition of a viscosity reducer diminishes the reactant concentration in the sealant, reducing the collision probability between the epoxy resin and the curing agent, and consequently prolonging the curing time. Excessive viscosity reducer may adversely impact the resin system's mechanical properties, while insufficient viscosity reducer can result in poor sealant fluidity. To ensure optimal sealant performance and construction efficiency, a 10% viscosity reducer concentration is employed for subsequent experiments.

The variations of viscosity with temperature for four types of epoxy resins within the range of 30–70 °C are presented in Fig. 5. It is observed that the viscosity of all resins sharply decreases with increasing temperature. The higher the initial viscosity, the greater the reduction rate. The sealant without any viscosity reducer exhibits a viscosity decrease from 865.53 mPa·s at 30 °C to 30.14 mPa·s at 70 °C, representing a 96.52% reduction. The sealant with 15% viscosity reducer shows a decrease from 118.71 mPa·s at 30 °C to 17.62 mPa·s at 70 °C, a 85.16% reduction. These results indicate that the effectiveness of viscosity reducers is more pronounced at lower temperatures. Higher temperatures result in lower viscosity of the sealant, thereby enhancing its migration capability within the wellbore system.

3.2. Sealant compressive strength

In compressive strength testing, stress-strain curves were obtained for conventional cement and epoxy resin. Fig. 6 shows the stress-strain curve for epoxy resin with 30% curing agent and cement. The cement abruptly fractured at a stress of 38.46 MPa,

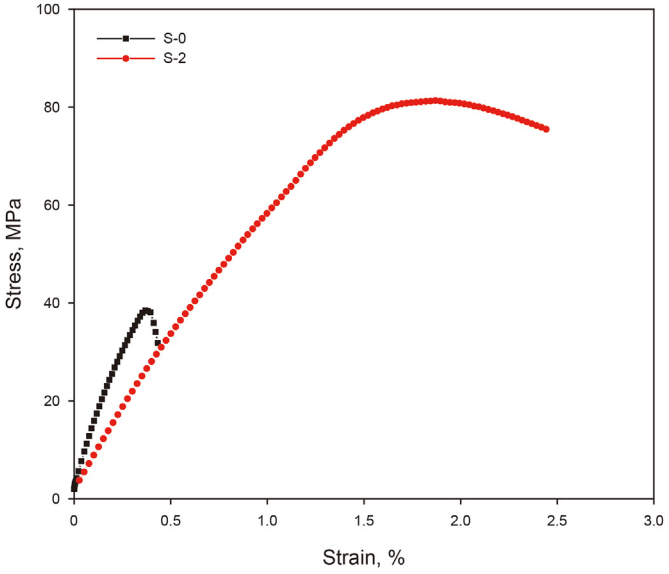

Fig. 6. Stress-strain curves of conventional cement and epoxy resins.

terminating the experiment. The stress-strain curve displayed a steep slope, following the mechanical deformation characteristics of brittle materials. S-2 samples gradually decreased in strength after reaching the peak point, while epoxy resin maintained residual strength and continued to bear a load. Throughout the entire process, epoxy resin exhibited strong elastic-plastic characteristics. With increasing stress, the strain of epoxy resin gradually increased, particularly exhibiting significant plastic properties under high stress. Even at the ultimate stress of epoxy resin, the sample did not shatter. It can be concluded that the mechanical deformation ability of epoxy resin is far superior to that of cement.

Fig. 7 presents the results of compressive strength tests performed on epoxy resin and cement at 3 and 14 days. At both 3 and 14 days, the compressive strengths of the epoxy resin incorporating three curing agents surpassed those of conventional cement. Cement exhibited a compressive strength of 32.53 MPa at 3 days and 38.46 MPa at 14 days, whereas epoxy resin demonstrated

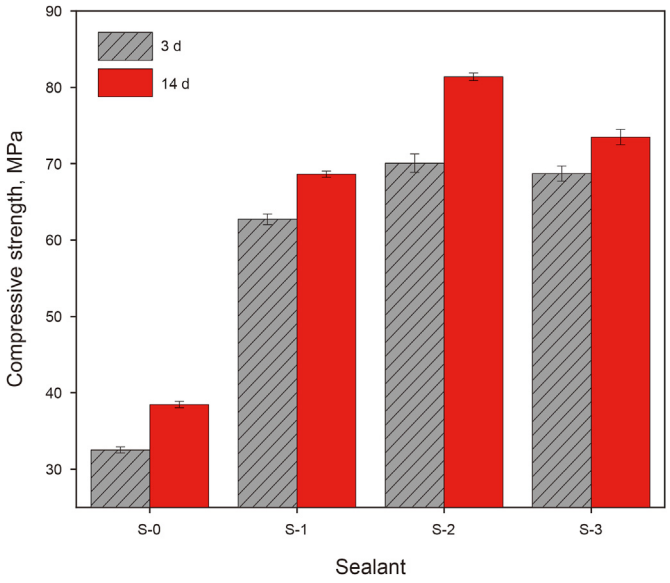

Fig. 7. Compressive strength of the cement and epoxy resin.

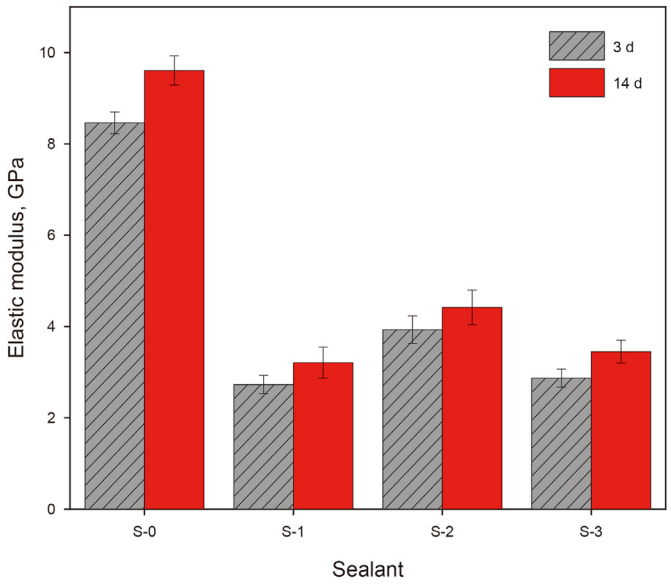

Fig. 8. Elastic modulus of the cement and epoxy resin.

compressive strengths ranging from 62.72 to 70.07 MPa and 68.63–81.37 MPa, respectively. The S-2 sample, containing 40% curing agent, exhibited the highest compressive strength, with values of 70.07 MPa at 3 days and 81.37 MPa at 14 days. At 3 and 14 days, the compressive strength of epoxy resin was 2.15 and 2.12 times higher than that of cement, respectively. The curing performance of epoxy resin is significantly affected by the amount of curing agent present. Electrophilic addition transpires between the hydroxyl group in the curing agent and the epoxy group in the resin. The resin's compressive strength is directly proportional to the quantity of curing agent introduced. It is noteworthy that the compressive strength of S-3 was lower than that of S-2 in both the 3 and 14-day tests. This can be attributed to the increased D230 content, which enlarges the space between cross-linking points, consequently leading to a decrease in the system's cross-linking density and ultimately reducing the system's cohesive strength and compressive strength.

3.3. Elastic modulus

In assessing the influence of curing agents on the mechanical properties of resin systems, the elastic modulus serves as a crucial parameter. A higher elastic modulus value indicates reduced elasticity, whereas a lower elastic modulus is more desirable for ensuring effective sealing in the wellbore annulus. Fig. 8 illustrates the elastic modulus of cement and epoxy resin. Both materials exhibit a rising trend in elastic modulus as curing time progresses. Among the epoxy resin samples, S-2 demonstrates the highest elastic modulus at 3 and 7 days, registering values of 3.93 MPa and 4.42 MPa, respectively. Conversely, S-1 exhibits the lowest elastic modulus at 3 and 7 days, with values of 2.73 and 3.21 MPa, respectively. At 3 and 14 days, the elastic modulus of cement is 3.09 and 2.99 times greater than that of S-1, respectively. As the elastic modulus is the stress-to-strain ratio, the lower elastic modulus of the epoxy resin can primarily be attributed to its increased deformation capacity, reflecting the resin's inherent flexibility.

3.4. Brittleness index

The ratio of compressive strength to flexural strength of cement, referred to as the brittleness index, reflects the toughness of the material. Fig. 9 illustrates the brittleness index of conventional cement and epoxy resin, which gradually decreased with curing time for both materials. As time progressed, the porosity of cement decreased and its internal structure became denser, resulting in a reduction of the brittleness index. It should be noted, however, that the brittleness index of cement was greater than that of epoxy resin. At 14 days, the brittleness index of S-0 was 7.61, while that of S-2 was 3.42. A smaller brittleness index indicated greater toughness of the epoxy resin. With an increase in the content of the curing agent, the brittleness index of the epoxy resin decreased, although the reduction gradually became less pronounced.

3.5. Tangential shear strength and normal shear strength

After 14 days of curing, the tangential shear strength of cement

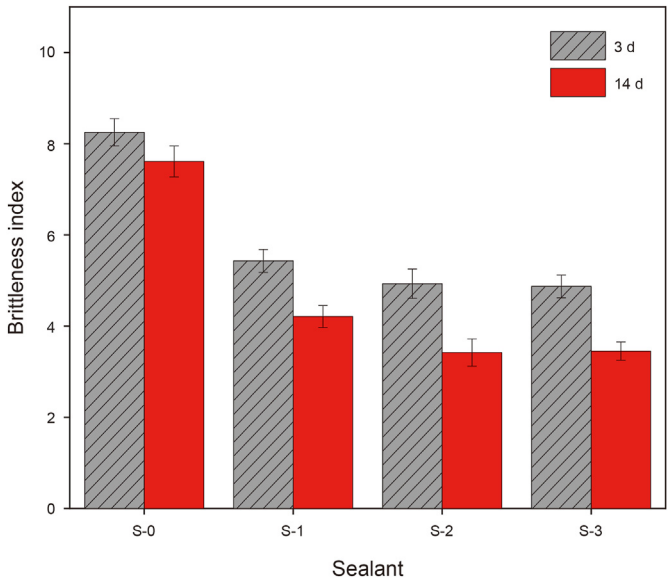

Fig. 9. Brittleness index of conventional cement and epoxy resin.

and epoxy resin samples generally exhibited higher values than those observed after 3 days, as illustrated in Fig. 10. Except for cement sample S-0, all other samples demonstrated high tangential shear strength. The tangential shear strength of S-1 reached 15.92 and 16.99 MPa after 3 and 14 days, respectively, representing a 200.00% and 166.67% enhancement compared to the conventional group S-0. As the curing agent content increased, the tangential shear strength of S-2 rose to 18.05 and 20.17 MPa. However, S-3 experienced a decline in comparison to S-2, registering values of 18.03 and 19.11 MPa, respectively.

Fig. 11 shows the normal shear strength results for cement and epoxy resin samples. The overall trend in normal shear strength mirrored that of the tangential shear strength. The normal shear strength of cement and epoxy resin samples following 14 days of curing was generally superior to that observed after 3 days. S-0 exhibited the lowest normal shear strength at both 3 and 14 days, with values of 3.67 and 5.67 MPa, respectively. The normal shear strength of S-2, containing 30% curing agent, was the highest, registering a 274.55% and 182.35% increase compared to the conventional group S-0 and reaching values of 13.73 and 16.00 MPa, respectively. The interfacial bond strength between the epoxy resin and casing steel demonstrates a stronger resistance to shear and tensile forces, necessitating greater force to initiate tangential and normal shear failures. This outstanding bonding performance can effectively repair SCP while enhancing the stability and sealing of wellbore annulus structures.

3.6. Sealant injection ability

The injectivity of sealant is critical in determining the volume and transport distance into the wellbore annulus. Injection experiments were conducted utilizing 0.5 mm-wide cracked cemented cores to investigate the sealant's injectivity, as illustrated in Fig. 12. The injection volumes for both epoxy resin and cement slurry were maintained at 0.5 PV. While injecting water, the pressure remained stable at approximately 0.76 kPa, indicating complete water entry into the crack and minimal water absorption by the cement matrix. As the sealant injection progressed, the injection pressure gradually increased for the three types of epoxy resins tested (S-1, S-2, and S-3), with injection pressures of 0.025, 0.054, and 0.075 MPa, respectively. The small disparities in injection pressure arose from varying curing agent content in the three solutions. As the curing agent increased, the epoxy resin's fluidity exhibited a minor decrease, suggesting that the epoxy resin's viscosity is predominantly influenced by the viscosity reducer, and the differences in fluidity among epoxy resins with identical viscosity reducer concentrations are relatively minimal. Conversely, during the cement slurry injection process, the injection pressure rapidly escalated to 2.61 MPa within a brief period, approximately 48.49 times higher than the epoxy resin. This increase can be attributed to the cement's limited transportability within the crack. The cement slurry, being a suspension containing solids, is prone to compression when traversing narrow cracks, leading to elevated inertia forces and heightened injection resistance. As the injection duration extends, viscous force gradually becomes the primary source of energy consumption during fluid flow. Consequently, as the cement's transport depth increases, the viscous force also intensifies, resulting in a continuous augmentation of the injection pressure gradient.

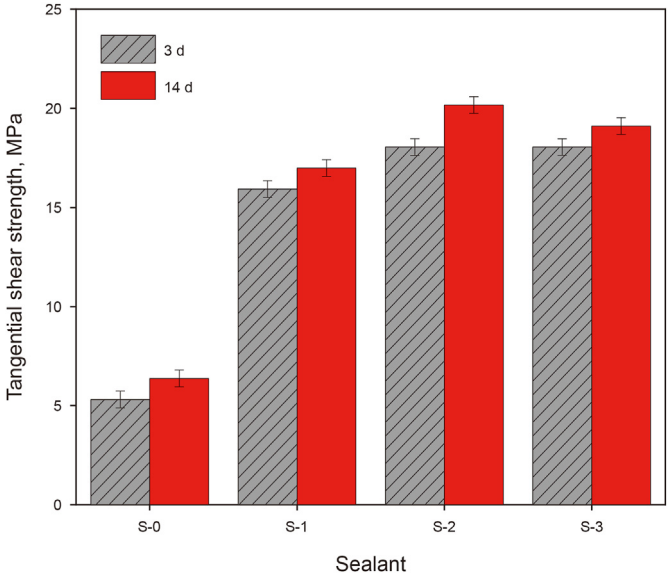

Fig. 10. Tangential shear strength of the cement and epoxy resin.

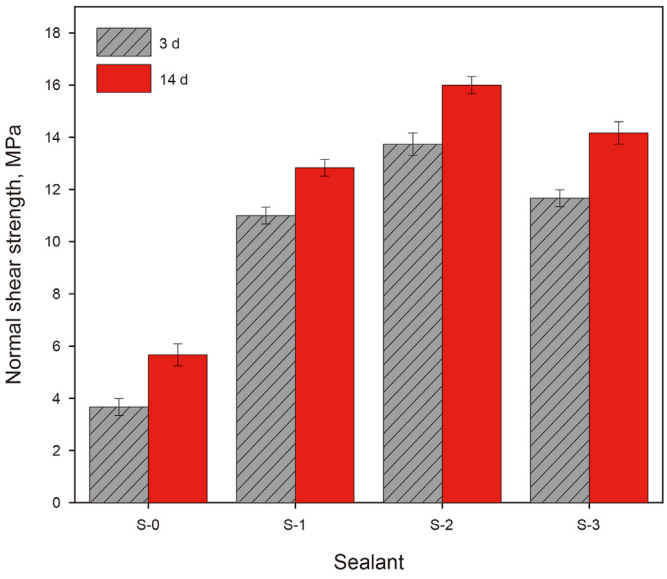

Fig. 11. Normal shear strength of the cement and epoxy resin.

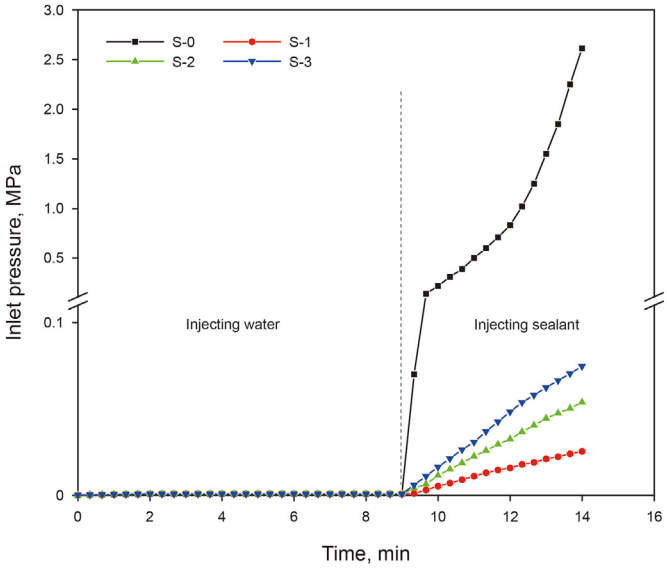

Fig. 12. Injection pressure of the cement and epoxy resin through 0.5 mm crack.

3.7. Sealant plugging ability

After the sealant had cured, a second water injection experiment was performed on the cement core. Fig. 13 presents the specific results. The injection pressure exhibited a consistent trend across different samples, characterized by a substantial increase followed by a sudden decline after reaching the peak. The pressure peak for S-0 was a mere 3.73 MPa before experiencing a sharp drop, indicating subpar plugging capability. The injection pressure peak of S-1 surpassed that of cement, reaching 5.37 MPa. The injection pressure peaks for samples S-2 and S-3 were both elevated, at 7.53 and 6.55 MPa, respectively. It is worth noting that the peak pressures of S-1, S-2, and S-3 were 1.44, 2.02, and 1.75 times of cement, respectively. In comparison to cement sealant, the epoxy resin sealant exhibited superior adhesion to cement crack surfaces and could withstand greater impact forces. Simultaneously, as the curing agent content increased, the epoxy resin's plugging capability initially improved and then declined, as corroborated by the epoxy resin shear strength results. The plugging ability displayed a positive correlation with shear strength, signifying that greater shear strength equates to enhanced plugging ability. The stable pressure of S-0 was a mere 0.12 MPa, while the stable pressures of S-1, S-2, and S-3 were 0.53, 1.26, and 0.93 MPa, respectively, representing increases of 4.42, 10.53, and 7.75 times of S-0. This observation implies that both cement and epoxy resin sealants were dislodged from the crack-bonding surfaces, forming water-channelling pathways. Nevertheless, the epoxy resin retained substantial plugging capacity, enabling it to continue plugging cracks in the cement core to a certain extent.

After the plugging experiment, the samples were subjected to an opening along the direction of the crack using a press machine. The loading force of the cement-plugged core was 3.4 kN, while that of the epoxy resin-plugged core was 15.7 kN. Fig. 14 shows the surface overview photos of the cracks of samples S-0 and S-2. For the S-0 sample, the cement slurry was evenly distributed in the crack, and the front edge exhibited piston-type advancement. Only a small amount of cement slurry could be seen on the gasket. In the S-2 sample, there are three aspects worth noting. Firstly, a thin layer of epoxy resin was unevenly distributed in the red line area. At the injection side, the epoxy resin filled the crack and was injected along the direction of the cement core into the crack. This is due to the low viscosity of the epoxy resin, exhibiting non-pistoning movement in the crack. Secondly, it is clear that the epoxy resin adhered to the gasket, indicating that it not only moved along the pre-made crack but also penetrated the gasket and the cement core. In particular, the traces of the resin penetrating along the gasket direction were found in the green frame, confirming the epoxy resin's strong flowability and ability to penetrate microcracks. At the injection side, it can be observed that the upper part of the cement core was broken, and a small part was tightly bonded to the lower part of the core by the epoxy resin. This demonstrates that the epoxy resin tightly bonded the two halves of the core together, with extremely high shear strength and forcing the cement core matrix to fracture.

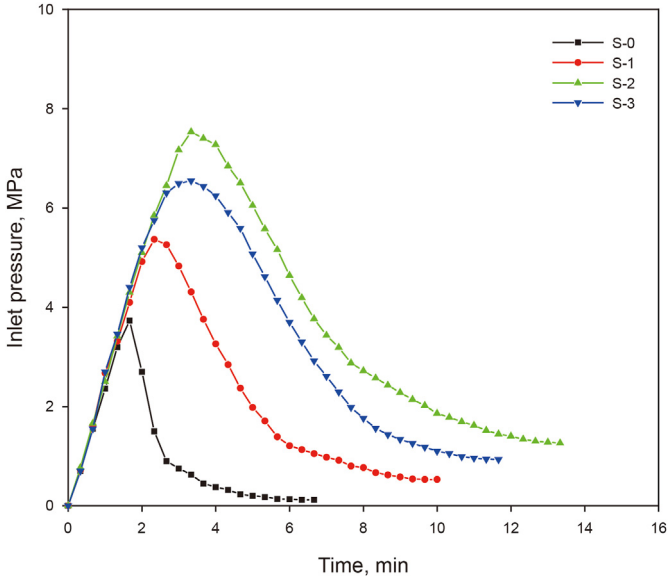

Fig. 13. Plugging pressure of the cement and epoxy resin in a 0.5 mm wide crack.

Fig. 15 presents the breakthrough pressures of 0.2 and 0.5 PV sealants after 3 days of curing in cement cores with crack widths of 0.5 and 2 mm. Under the condition of a 0.5 mm crack width, S-1, S-2, and S-3 exhibit superior breakthrough pressures compared to S-0. For example, the breakthrough pressure of S-0 at 0.2 PV is 1.29 MPa, while that of S-0 at 0.5 PV is 3.73 MPa. In comparison to the conditions of 0.2 and 0.5 PV, epoxy resin sealants demonstrate enhanced plugging ability, with breakthrough pressures ranging from 1.85 to 2.51 MPa and 5.37–7.53 MPa, respectively. These results suggest that epoxy resin has adequately filled the cement cracks, effectively connecting and compacting with the cement cracks, thereby improving the sealant interface's plugging capability. In contrast, the inferior fluidity of the cement slurry injected into cracks results in weakened bonding capacity.

Considering the diverse sizes and shapes of cracks in wellbore annulus, it is crucial to investigate the effect of crack size on sealants for remedial operations. The breakthrough pressures at different crack widths were compared. At a 0.5 mm crack width, the breakthrough pressure of S-0 is 3.73 MPa, whereas, at a 2 mm crack width, the breakthrough pressure decreases to 1.57 MPa. After plugging 2 mm cracks with epoxy resin, the maximum breakthrough pressure still reaches 5.47 MPa, 3.48 times of cement. Both cement and epoxy resin sealants exhibit a decreasing trend in breakthrough pressure as the crack width increases. Despite the enlargement of crack width, the plugging capability of the resin remains relatively stable, consequently forming a high-strength seal.

To evaluate the plugging ability of the sealant within the cracks, two parameters commonly employed in conventional oil displacement experiments are introduced: the residual resistance coefficient (*Frr*) and the plugging efficiency (*E*). Frr characterizes the sealant's capacity to decrease the permeability of the cracks; a higher value indicates a superior plugging performance of the sealant. *Frr* is defined as the ratio of the water-phase permeability of the cracks before and after the sealant injection. Moreover, *Frr* can be expressed in terms of stable water injection pressure, with the specific formula as follows:

$$Frr = \frac{P_1}{P_2} \tag{2}$$

where P_1 is the water flooding stable pressure before sealant injection, and P_2 is the water flooding stable pressure after sealant injection.

The plugging efficiency (E) is the percentage of water phase permeability reduction of the crack after injecting the sealant. The expression for E is given as:

$$E = \left[1 - \left(\frac{1}{Frr}\right)\right] * 100 \tag{3}$$

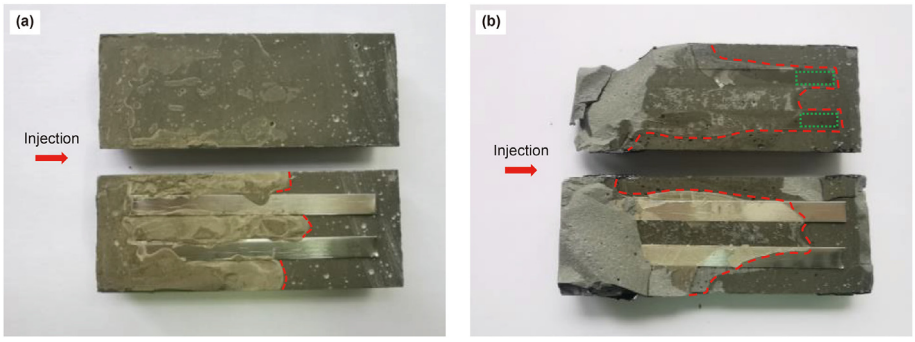

Fig. 14. Surface images of the cement and epoxy resin in the cracks after the experiment. (**a**) Morphology of cement in the crack. (**b**) Morphology of epoxy resin in the crack.

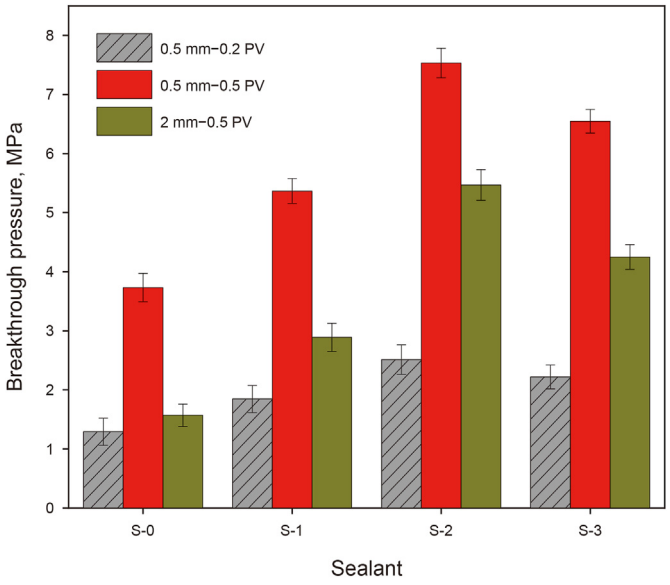

Fig. 15. Effect of crack width and injection PV on breakthrough pressure of cement and epoxy resin.

Table 1 presents the *Frr* and *E* values for various sealants injected into cement cores containing cracks. As the curing agent content increases, both *Frr* and *E* initially rise and subsequently decline. This suggests that augmenting the curing agent content is beneficial; however, its quantity should be regulated when employing epoxy resin for fluid plugging applications. It is worth noting that the *E* values for S-1, S-2, and S-3 all surpass 99.9%, which is substantially higher than the *E* value for S-0. Moreover, as the crack width expands from 0.5 to 2 mm, the *Frr* and *E* values for all four sealants diminish to varying extents, indicating that the plugging capability of both cement and epoxy resin within cement cracks weakens as the crack width increases. Overall, epoxy resin demonstrates considerable potential as an alternative to conventional cement for SCP remediation efforts.

Table 1
Frr and *E* of cement and epoxy resin.

Crack-injection volume	Plugging parameter	S-0	S-1	S-2	S-3
0.5 mm–0.2 PV	*Frr*	75	199	416	408
	E, %	98.67	99.50	99.76	99.75
0.5 mm–0.5 PV	*Frr*	158	697	1662	1224
	E, %	99.37	99.86	99.94	99.92
2 mm–0.5 PV	*Frr*	98	473	1143	893
	E, %	98.98	99.79	99.91	99.89

3.8. Crack permeability

Fig. 16 illustrates the permeability of the 0.5 mm width crack before and after plugging. As the injection volume of S-0 increases from 0.2 to 0.5 PV, the permeability declines from 0.49 to 0.23 D. With a 2.5-fold increase in injection volume, the permeability decreases by 53.06%, signifying that a larger injection volume of cement leads to improved crack plugging. However, as depicted in Fig. 11, a rise in injection volume results in a sharp increase in cement injection pressure, indicating that cement's transport capability within cracks is constrained, thereby severely limiting its injection volume and plugging efficiency. Conversely, after plugging the cracks with resin, the permeability diminishes to a range of 0.02–0.18 D, effectively blocking the crack pathway. A reduction in resin quantity leads to a decrease in plugging capability. As the curing agent content increases, the resin's ability to reduce crack permeability first strengthens and then weakens, albeit with a minor difference. After plugging with a 0.5 PV sealant, the permeability of S-2 is only 0.02 D, which constitutes 9.49% of the permeability post-plugging with S-0. Overall, epoxy resin demonstrates superior crack-plugging efficiency compared to conventional cement.

4. Conclusions

(1) The mechanical properties of epoxy resin are optimized with a curing agent content of 30%, resulting in superior compressive strength, tangential shear strength, and normal

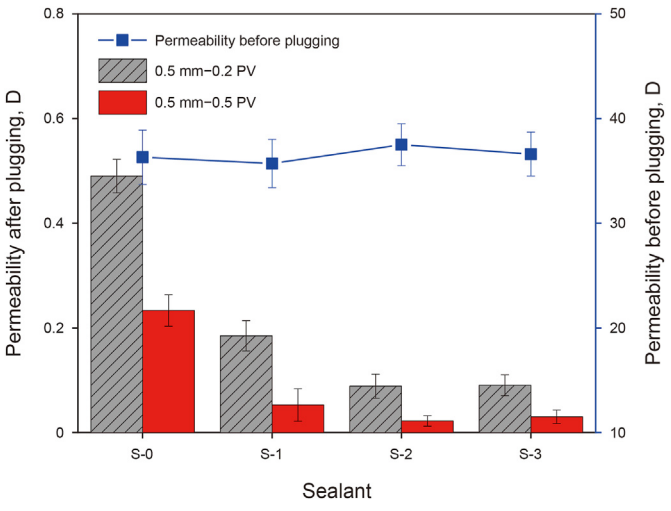

Fig. 16. Permeability of 0.5 mm crack before and after plugging.

shear strength compared to conventional cement. The epoxy resin demonstrates lower elastic modulus and Brittleness index than conventional cement, while exhibiting excellent compressive strength, toughness, and interfacial bond strength.

(2) At a 0.5 mm crack width, the injection pressure of cement is 48.49 times higher than that of epoxy resin. Epoxy resin, with excellent seepage capacity, can effectively penetrate narrow cracks and is an ideal material for repairing small cracks.

(3) Epoxy resin exhibits a higher breakthrough pressure than cement at a crack width of 0.5 mm, with a permeability of only 9.49% that of cement. Even with an increased crack width of 2 mm, epoxy resin is still effective in sealing crack and preventing fluid flow. Epoxy resin presents a viable alternative to Portland cement for addressing oil and gas well casing sustained pressure (SCP) challenges.

CRediT authorship contribution statement

Guang-Yao Leng: Conceptualization, Data curation, Methodology, Writing – original draft. **Wei Yan:** Data curation, Investigation, Resources. **Hai-Mu Ye:** Investigation, Supervision. **Er-Dong Yao:** Investigation, Writing – review & editing. **Ji-Bin Duan:** Data curation, Validation. **Zheng-Xian Xu:** Investigation, Writing – review & editing. **Ke-Pei Li:** Data curation, Validation. **Jing-Ru Zhang:** Writing – original draft. **Zhong Li:** Resources, Supervision.

Declaration of competing interest

All authors declare that no conflict of interest exists.

Acknowledgements

This work was funded by the National Natural Science Foundation Project (Grant No. 52274015).

References

Abdulfarraj, M., Imqam, A., 2020. The potential of using micro-sized crosslinked polymer gel to remediate water leakage in cement sheaths. J. Pet. Explor. Prod. Technol. 10, 871–881. https://doi.org/10.1007/s13202-019-00783-6.

Ahdaya, M., Imqam, A., 2019. Investigating geopolymer cement performance in presence of water based drilling fluid. J. Petrol. Sci. Eng. 176, 934–942. https://doi.org/10.1016/j.petrol.2019.02.010.

Ali, W., Al-Turki, F.A., Abbas, A., et al., 2022. Application of innovative resin system to improve wellbore integrity: case studies from Saudi Arabia. In: SPE Asia Pacific Oil & Gas Conference and Exhibition. https://doi.org/10.2118/210620-MS.

Alkhamis, M., Imqam, A., 2021. Sealant injectivity through void space conduits to assess remediation of well cement failure. J. Pet. Explor. Prod. Technol. 11, 2791–2804. https://doi.org/10.1007/s13202-021-01218-x.

Alkhamis, M., Imqam, A., 2018. New cement formulations utilizing graphene nano platelets to improve cement properties and long-term reliability in oil wells. In: SPE Kingdom of Saudi Arabia Annual Technical Symposium and Exhibition. https://doi.org/10.2118/192342-MS.

Alsaihati, Z.A., Al-Yami, A.S., Wagle, V., et al., 2017. An overview of polymer resin systems deployed for remedial operations in Saudi Arabia. In: SPE Kingdom of Saudi Arabia Annual Technical Symposium and Exhibition. https://doi.org/10.2118/188122-MS.

Al-Yami, A., Wagle, V., Jimenez, W.C., et al., 2019. Evaluation of epoxy resin thermal degradation and its effect on preventing sustained casing pressure in oil and gas wells. Arabian J. Sci. Eng. 44, 6109–6118. https://doi.org/10.1007/s13369-018-3651-y.

Cao, C., Bu, Y., Tian, L., et al., 2022. Epoxy resin-based cementing fluid produces a low elastic modulus cementing fluid system and enhances the cement–formation interface. Arabian J. Sci. Eng. 47, 11987–11998. https://doi.org/10.1007/s13369-022-06750-4.

Dahlem, J.E., Baughman, T., James, T., et al., 2017. Intervention and abandonment - riserless productive zone abandonment using epoxy resin. In: SPE Offshore Technology Conference. https://doi.org/10.4043/27847-MS.

Du, J., Zhou, A., Lin, X., et al., 2020. Revealing expansion mechanism of cement-stabilized expansive soil with different interlayer cations through molecular dynamics simulations. J. Phys. Chem. C 124, 14672–14684. https://doi.org/10.1021/acs.jpcc.0c03376.

Elyas, O., Alyami, A., Wagle, V., et al., 2018. Use of polymer resins for surface annulus isolation enhancement, in: all days. In: SPE Kingdom of Saudi Arabia Annual Technical Symposium and Exhibition. https://doi.org/10.2118/192266-MS.

Fan, J., Qu, Z., Guo, T., et al., 2022. Development of self-generated proppant based on modified low-density and low-viscosity epoxy resin and its evaluation. Petrol. Sci. 19 (5), 2240–2252. https://doi.org/10.1016/j.petsci.2022.05.009.

Gu, C., Li, X., Feng, Y., et al., 2022. Numerical investigation of cement interface debonding in deviated shale gas wells considering casing eccentricity and residual drilling fluid. Int. J. Rock Mech. Min. Sci. 158, 105197. https://doi.org/10.1016/j.ijrmms.2022.105197.

Guo, S., Bu, Y., Yang, X., et al., 2020a. Effect of casing internal pressure on integrity of cement ring in marine shallow formation based on XFEM. Eng. Fail. Anal. 108, 104258. https://doi.org/10.1016/j.engfailanal.2019.104258.

Guo, S., Luo, H., Tan, Z., et al., 2021a. Impermeability and interfacial bonding strength of TiO_2-graphene modified epoxy resin coated OPC concrete. Prog. Org. Coating 151, 106029. https://doi.org/10.1016/j.porgcoat.2020.106029.

Guo, S., Zhang, X., Chen, J., et al., 2020b. Mechanical and interface bonding properties of epoxy resin reinforced Portland cement repairing mortar. Construct. Build. Mater. 264, 120715. https://doi.org/10.1016/j.conbuildmat.2020.120715.

Guo, S., Zhang, X., Ren, J., et al., 2021b. Preparation of TiO_2/epoxy resin composite and its effect on mechanical and bonding properties of OPC mortars. Construct. Build. Mater. 272, 121960. https://doi.org/10.1016/j.conbuildmat.2020.121960.

Huseien, G.F., Sam, A.R.M., Faridmehr, I., et al., 2021. Performance of epoxy resin polymer as self-healing cementitious materials agent in mortar. Materials 14, 1255. https://doi.org/10.3390/ma14051255.

Jelena, T., Martin, R., Erik, L., et al., 2016. Remediation of leakage through annular cement using a polymer resin: a laboratory study. Energy Proc. 86, 442–449. https://doi.org/10.1016/j.egypro.2016.01.045.

Jones, P.J., Karcher, J.D., Ruch, A., et al., 2014. Rigless operation to restore wellbore integrity using synthetic-based resin sealants. In: SPE/EAGE European Unconventional Resources Conference and Exhibition. https://doi.org/10.2118/167759-MS.

Li, M., Zhou, F., Wang, B., et al., 2022. Numerical simulation on the multiple planar fracture propagation with perforation plugging in horizontal wells. Petrol. Sci. 19 (5), 2253–2267. https://doi.org/10.1016/j.petsci.2022.05.004.

Manceau, J.C., Hatzignatiou, D.G., De Lary, L., et al., 2014. Mitigation and remediation technologies and practices in case of undesired migration of CO_2 from a geological storage unit—current status. Int. J. Greenh. Gas Control 22, 272–290. https://doi.org/10.1016/j.ijggc.2014.01.007.

Marfo, S.A., Appah, D., Joel, O.F., et al., 2015. Sand consolidation operations, challenges and remedy. In: SPE Nigeria Annual International Conference and Exhibition. https://doi.org/10.2118/178306-MS.

Ren, J., Guo, S., Zhao, T., et al., 2020. Constructing a novel nano-TiO_2/Epoxy resin composite and its application in alkali-activated slag/fly ash pastes. Construct. Build. Mater. 232, 117218. https://doi.org/10.1016/j.conbuildmat.2019.117218.

Retnanto, A., Yrac, R., Cardena, N., et al., 2023. Assessment of resin systems as solution for well integrity challenge in carbonate reservoirs. J. Pet. Explor. Prod. Technol. https://doi.org/10.1007/s13202-023-01608-3.

Rusch, D.W., 2004. Subsea leaks cured with pressure-activated sealant. In: SPE Asia Pacific Oil and Gas Conference and Exhibition. https://doi.org/10.2118/88566-MS.

Sanabria, A.E., Knudsen, K., Leon, G.A., 2016. Thermal activated resin to repair casing leaks in the middle east. In: SPE Abu Dhabi International Petroleum Exhibition & Conference. https://doi.org/10.2118/182978-MS.

Schütz, M.K., Baldissera, A.F., Coteskvisk, P.M., et al., 2018. Chemical degradation of reinforced epoxy-cement composites under CO_2-rich environments. Polym. Compos. 39, E2234–E2244. https://doi.org/10.1002/pc.24589.

Schütz, M.K., dos Santos, L.M., Coteskvisk, P.M., et al., 2019. Evaluation of CO_2 attack in wellbore class G cement: influence of epoxy resins, composites and minerals as additives. Greenhouse Gas Sci Technol 9, 1276–1287. https://doi.org/10.1002/ghg.1928.

Skadsem, H.J., 2022a. Characterization of annular cement permeability of a logged well section using pressure–pulse decay measurements. J. Energy Resour. Technol. 144, 053004. https://doi.org/10.1115/1.4053709.

Skadsem, H.J., 2022b. Fluid migration characterization of full-scale annulus cement sections using pressure-pulse-decay measurements. J. Energy Resour. Technol. 144 (7), 073005. https://doi.org/10.1115/1.4052184.

Song, J., Xu, M., Tan, C., et al., 2022. Study on an epoxy resin system used to improve the elasticity of oil-well cement-based composites. Materials 15, 5258. https://doi.org/10.3390/ma15155258.

Todd, L., Cleveland, M., Docherty, K., et al., 2018. Big problem-small solution: nanotechnology-based sealing fluid. In: SPE Annual Technical Conference and Exhibition. https://doi.org/10.2118/191577-MS.

Wasnik, A., Mete, S., 2005. Application of resin system for sand consolidation, mud-loss control, and channel repairing. In: SPE International Thermal Operations and Heavy Oil Symposium. https://doi.org/10.2118/97771-MS.

Zhu, H., Lin, Y., Zeng, D., et al., 2012. Calculation analysis of sustained casing pressure in gas wells. Petrol. Sci. 9, 66–74. https://doi.org/10.1007/s12182-012-0184-y.